Click chemistry for photonic applications: triazole-functionalized platinum(II) acetylides for optical power limiting

Robert Westlund,[a] Eirik Glimsdal,[b] Mikael Lindgren,[b] Robert Vestberg,[c] Craig Hawker,[c] Cesar Lopes[d] and Eva Malmström*[a]

Three different triazole-containing platinum(II) acetylide compounds were synthesized by click chemistry and evaluated for their use in optical power limiting (OPL) applications. The triazole unit was incorporated at three different positions within, or at the end of, the conjugation path of the chromophore. The aim is to explore the possibilities of using click chemistry to prepare dendronized chromophores, and to evaluate how the triazole structure affects the photophysical properties and the optical power limiting abilities of these acetylide compounds. It is shown that the concept of click chemistry can be used to attach branched monomer units to ethynyl-phenyl arms by Huisgen 1,3-dipolar cycloaddition, forming triazole units within the chromophore. Photophysical characterization of these triazole-containing materials shows an absorption maximum within the UV-A region and emission through both fluorescence and phosphorescence. Bright phosphorescence was emitted from argon purged samples, and decay measurements thereof showed triplet lifetimes of up to 100 μs. The results from the photophysical characterization suggest that the triazole does break the conjugation path, and in order to gain maximum optical limiting the triazole needs to be placed at the end of the conjugation. All three investigated triazole-containing platinum(II) acetylides show good optical power limiting at 532 nm (10 ns pulse, f/5 set-up, 2 mm cells). The most efficient compound, with the triazole positioned at the end of the conjugation, reaches a defined clamping level of 2.5 μJ for a sample with a concentration of 50 mM in THF and a linear transmission above 80% at 532 nm. These data can be compared to the OPL properties of Zn-based porphyrins or derivatized thiophenes, reaching clamping levels of 6–15 μJ.

Introduction

The use of lasers has increased over the years and likewise there has also been a rapid development of powerful wavelength-agile lasers.[1] Consequently, there is an increasing interest in research and development of new, efficient optical power limiting (OPL) materials[2–4] in order to meet safety requirements and potential laser threats. Nonlinear optical (NLO) limiting materials[5,6] can be used to reduce the transmission of high-intensity light. There are several mechanisms that may give rise to nonlinear absorption, for example two photon absorption (TPA)[7–9] or excited state absorption (ESA).[10,11] Organic chromophores consisting of π-conjugated aromatics can possess such NLO properties and novel synthetic routes are being developed to enhance the OPL function and to simultaneously add additional functionalities, for example, increase of π-conjugation length,[3,12] incorporating heavy atoms to gain spin–orbit coupling for enhanced

intersystem crossing (ISC),[12–15] addition of donor/acceptor moieties,[7,16] dendritic capping,[17,18] or sol–gel processing units.[19,20] NLO chromophores suitable for sensor protection require certain factors to be considered. Firstly, the chromophore must possess efficient nonlinear absorption for high-intensity light, thus limiting the transmission of high-intensity light to a low level, while the transmission of low-intensity light is kept high. Secondly, the nonlinear response must be fast, within picoseconds.[2,3]

Earlier studies pioneered by McKay and Staromlynska et al.,[21–23] and by the present authors,[17,18] have shown that platinum(II) acetylides possess good optical power limiting properties due to efficient excited state absorption. It has also been shown that by adding dendritic substituents to the Pt chromophore, the OPL properties can be enhanced greatly due to increased site isolation.[18] The larger the dendritic substituents on the chromophore, the better clamping levels could be reached. Thus, the dendrimer here provides the ability to create a micro-environment for the core-molecule,[24] and acts as a "molecular bumper", minimizing quenching of excited triplet states by collisions with other solute molecules or oxygen.[18,25]

Click chemistry reactions are usually defined as regiospecific reactions resulting in easily isolated products in quantitative yields.[26] Triazole formation through 1,3-dipolar cyclo-addition[27] of azides and alkynes is a commonly used click

[a]KTH Fibre and Polymer Technology, Royal Institute of Technology, Teknikringen 56-58, SE-100 44 Stockholm, Sweden. E-mail: mave@polymer.kth.se; Fax: +46 8790 8283; Tel: +46 8790 8273
[b]Department of Physics, Norwegian University of Science and Technology, NO-7491 Trondheim, Norway
[c]Materials Research Laboratory, University of California, Santa Barbara, CA 93106, USA
[d]Department of Functional Materials, Swedish Defence Research Agency, SE-581 11 Linköping, Sweden

reaction and it can be used successfully to build up dendrimers,[28,29] or dendronized polymers[30] due to mild reaction conditions and compatibility with a wide variety of functional groups. In addition, the introduced triazole ring is chemically and thermally stable while also possessing a large dipole moment, features that may be beneficial in OPL applications. The increased number of end-groups in dendrimers is especially useful in the preparation of solid state materials where functionalization of the chromophore is necessary in order to obtain well dispersed hybrid materials.[19] The aim of this study has been to investigate the ability to use 'click chemistry' in order to synthesize platinum(II) acetylides functionalized with first generation 2,2-bis(methylol)propionic acid (bis-MPA) dendrons, targeted for OPL. Specifically, we used the triazole-forming click reaction to attach branched monomer units to ethynyl-phenyl arms to prepare a set of model chromophores. The motive for using click chemistry was to efficiently introduce the required molecular building blocks for construction of reactive OPL derivatives while at the same time introducing functional triazole units. The advantage of using click chemistry is that the dendritic units may be pre-synthesized and then added to the phenyl-ethynyl ligands. Previously, dendrons were grown divergently from the acetylide arms[18] and hence, for each generation being synthesized, precious amounts of acetylide arms were lost due to chromatographic purification.

By employing click chemistry, three different structures of platinum(II) acetylides containing triazole units were successfully synthesized. Herein, we also investigate the effect of the triazole unit on the photophysical properties and the OPL performance of these modified platinum(II) acetylides.

Experimental

^1H and ^{13}C NMR spectra were recorded on a Bruker AM 400 using acetone-d_6, DMSO-d_6 or CDCl$_3$ as solvent. The solvent signal was used as internal standard. Fourier transformed infrared spectra (FTIR) were recorded on a Perkin-Elmer Spectrum 2000 FT-IR instrument using a MKII Golden Gate, single reflection ATR system.

Steady state absorption spectra were recorded using a Shimadzu UV-1601PC Spectrometer. Measurements were performed with samples diluted to 10 μM in tetrahydrofuran solvent (THF, ⩾99.5% spectrophotometric grade, from Sigma-Aldrich) using 10 mm quartz cells (Hellma Precision). Luminescence spectra and excited state lifetimes were recorded using a Jobin Yvon IBH FluoroCube photon-counting spectrometer as detection unit. A titanium : sapphire laser (Coherent Mira 900-f) was used as radiation source in all experiments. The fundamental output from the mode-locked laser is pulses of approximately 200 femtosecond duration and 76 MHz pulse repetition frequency (prf). The pulse repetition frequency was controlled by an acousto-optic modulator (Coherent 9200 Pulse Picker) between 9 kHz and 4.75 MHz. Single-photon excitation experiments were performed by frequency doubling of the fundamental output, to below 400 nm using a SHG crystal (Inrad Ultrafast Harmonic Generation System, Model 5-050). A schematic view of the experimental set-up is shown in Fig. 1. Fluorescence and phosphorescence
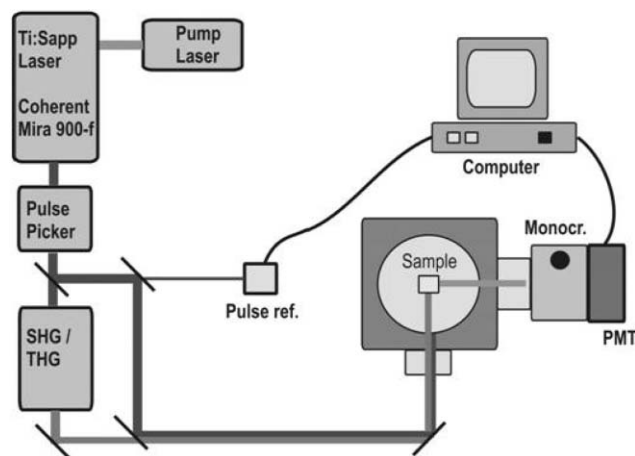
Fig. 1 Experimental set-up for time-resolved and luminescence measurements. The frequency doubled (SHG) beam (exiting SHG/THG) is used for single-photon excitation, and the fundamental beam (exiting the pulse picker) for two-photon measurements.

emission lifetimes were measured using the luminescence spectrometer in time-correlated single photon counting (TC-SPC) mode. The IBH TB-01 module (optical trigger) was used as time-reference in those experiments, using a thin glass wedge to take out a small part of the fundamental. Pseudo-steady state emission spectra were recorded by scanning the monochromator in front of the photomultiplier tube (PMT).

Fluorescence quantum efficiencies were found from relative measurements in low concentration samples (absorption < 0.1 OD) by comparing the results to a known reference material, in a similar way to the method of Williams et al.,[31] and hence, the absolute quantum yield value could be calculated. The chromophore coumarin 110 (C110) was used as both quantum efficiency reference material, and as a reference in the two-photon measurements. C110 has previously been characterized and found to have a quantum yield of 0.60 in THF solvent, when compared to the well known quantum yield reference quinine sulfate.[32] The two-photon absorption cross section of C110 was found to be approximately 7 GM at 720–760 nm (1 GM = 10^{-50} cm^4 s photon^{-1}).

Optical limiting measurements were conducted in a f/5 set up with a frequency doubled Nd : YAG laser operating at 10 Hz, delivering 5 ns pulses. Measurements were performed using 2 mm quartz cells and THF as solvent (50 mM solutions).

MALDI-TOF spectra were recorded on a Bruker UltraFlex MALDI-TOF mass spectrometer with a SCOUT-MTP ion source (Bruker Daltronics) equipped with a nitrogen laser (337 nm), a gridless ion source and a reflector. A THF solution of 9-nitroanthracene and trifluoroacetic acid sodium salt was used as matrix.

Materials

2,2-Bis(methylol)propionic acid (bis-MPA) was supplied by Perstorp AB, Sweden. The acetonide protected bis-MPA and the anhydride were synthesized according to Malkoch et al.[33] Cu(PPh$_3$)$_3$Br,[34] 4-(4-iodophenyl)-2-methyl-3-butyn-2-ol,[18] Pt(PBu$_3$)$_2$Cl$_2$ (trans configuration),[18] and 4-(dimethylamino)pyridinium 4-toluenesulfonate[35] (DPTS) were synthesized as

This journal is © The Royal Society of Chemistry 2008

J. Mater. Chem., 2008, **18**, 166–175 | 167

described previously. All other reagents were obtained from Aldrich and used as received.

Synthesis of chloro-functional bis-MPA (1). 3-Chloro-1-propanol (5.0 g; 52.9 mmol) and acetonide protected bis-MPA (11 g; 63.5 mmol) was dissolved in DCM. DPTS (3.11 g; 10.6 mmol) and N,N'-dicyclohexylcarbodiimide (DCC, 13.1 g; 63.5 mmol) were added and the reaction was stirred at room temperature for 24 h. DCC-urea was filtered off and the organic solution was extracted 3 times with Na_2CO_3 (10%) and once with brine. The organic phase was dried over $MgSO_4$ and purified by flash chromatography, starting with pure heptane and gradually increasing polarity to 20 : 80 ethyl acetate–heptane. Yield 66%. ^{1}H NMR (CDCl$_3$): δ 1.03 (s, 3H, –CH$_2$–C–CH$_3$), 1.27 (s, 3H, O–C–CH$_3$), 1.31 (s, 3H, O–C–CH$_3$), 2.03 (m, 2H, –CH$_2$–CH$_2$–O–), 3.54 (t, 2H, –CH$_2$–Cl), 3.55 (d, 2H, J = 12.0 Hz, –C–CH$_2$–O–), 4.08 (d, 2H, J = 12.0 Hz, –C–CH$_2$–O–), 4.19 (t, 2H, J = 6.0 Hz, –CH$_2$–CH$_2$–O–). ^{13}C NMR (CDCl$_3$): δ 18.43, 22.08, 25.29, 31.48, 42.29, 61.49, 66.06, 98.03, 174.07.

Azide-functional bis-MPA (2). Chloro-functional bis-MPA **1** (8.7 g; 34.7 mmol) was dissolved in 60 mL DMSO. Sodium azide (5.64 g; 86.9 mmol) was added and the reaction was stirred at 80 °C for 24 h. 10 mL of H_2O and 20 mL of ether were added. The water phase was removed and the organic phase was further extracted twice with water. The organic phase was dried over $MgSO_4$ and concentrated, yielding 98% of a clear liquid. ^{1}H NMR (CDCl$_3$): δ 1.11 (s, 3H, –CH$_2$–C–CH$_3$), 1.33 (s, 3H, O–C–CH$_3$), 1.36 (s, 3H, O–C–CH$_3$), 1.88 (m, 2H, –CH$_2$–CH$_2$–O–), 3.35 (t, 2H, –CH$_2$–N$_3$), 3.58 (d, 2H, J = 12.0 Hz, –C–CH$_2$–O–), 4.13 (d, 2H, J = 12.0 Hz, –C–CH$_2$–O–), 4.19 (t, 2H, J = 6.0 Hz, –CH$_2$–CH$_2$–O–). ^{13}C NMR (CDCl$_3$): δ 18.43, 21.98, 25.16, 28.10, 41.89, 48.00, 61.59, 66.00, 98.00, 174.02.

General procedure for triazole formation, exemplified with the synthesis of compound 3. Azide-functional bis-MPA **2** (2.04 g; 7.92 mmol) and 1,4-diethynyl benzene (1.0 g; 7.92 mmol) were dissolved in 20 mL THF. Cu(PPh$_3$)$_3$Br (0.74 g; 0.792 mmol) and diisopropyl ethylamine (DIPEA, 1.02 g; 7.92 mmol) were added and the reaction was stirred at room temperature for 24 h. Solvent was evaporated off and the crude reaction mixture was redissolved in DCM and extracted twice with NaHSO$_4$ (10%). The organic phase was dried with $MgSO_4$ and then purified with flash chromatography, eluting with hexane, gradually increasing to pure ethyl acetate. The product was obtained as a pale brown solid in 52% yield. ^{1}H NMR (CDCl$_3$): δ 1.11 (s, 3H, –CH$_2$–C–CH$_3$), 1.36 (s, 3H, O–C–CH$_3$), 1.44 (s, 3H, O–C–CH$_3$), 2.34 (m, 2H, –CH$_2$–CH$_2$–O–), 3.28 (s, 1H, –C≡C–H), 3.66 (d, 2H, J = 12.0 Hz, –C–CH$_2$–O–), 4.21 (d, 2H, J = 12.0 Hz, –C–CH$_2$–O–), 4.31 (t, 2H, J = 6.0 Hz, –CH$_2$–N), 4.61 (t, 2H, J = 6.0 Hz, –CH$_2$–CH$_2$–O–), 7.62 (d, 2H, J = 10.0 Hz, Ar–H), 7.82 (d, 2H, J = 10.0 Hz, Ar–H), and 8.09 (s, 1H, –N–CH–). ^{13}C NMR (CDCl$_3$): δ 18.31, 20.72, 26.71, 29.42, 42.20, 46.90, 61.05, 66.24, 83.44, 98.20, 99.97, 120.60, 121.76, 125.55, 130.79, 132.62, 146.94, 174.18.

General procedure for platinum coupling reaction, exemplified with the synthesis of Z1. Alkyne **3** (1.37 g; 3.57 mmol) and

Pt(PBu$_3$)$_2$Cl$_2$ (1.19 g; 1.79 mmol) were dissolved in 50 mL THF–triethylamine (TEA, 50 : 50). The reaction was heated to 60 °C and a catalytic amount of CuI was added. The reaction was stirred at 60 °C for 20 min and followed by TLC. When complete, solvents were evaporated off and the crude reaction mixture was redissolved in DCM and extracted twice with NaHSO$_4$ (10%). The organic phase was dried over $MgSO_4$ and purified by flash chromatography, eluting with ethyl acetate–heptane starting from 20 : 80 and gradually increasing to 70 : 30. The product was obtained as a pale yellow solid in 79% yield. ^{1}H NMR (CDCl$_3$): δ 0.86 (t, 18H, J = 8.0, –CH$_2$–CH$_3$), 1.07 (s, 6H, –CH$_2$–C–CH$_3$), 1.36 (s, 6H, O–C–CH$_3$), 1.44 (s, 6H, O–C–CH$_3$), 1.45 (m, 12H, –CH$_2$–CH$_3$), 1.56 (m, 12H, CH$_2$–CH$_2$–CH$_3$), 2.08 (m, 12H, –P–CH$_2$–), 2.28 (m, 4H, –CH$_2$–CH$_2$–O–), 3.61 (d, 4H, J = 12.0 Hz, –C–CH$_2$–O–), 4.15 (d, 4H, J = 12.0 Hz, –C–CH$_2$–O–), 4.16 (t, 4H, J = 6.0 Hz, –N–CH$_2$), 4.47 (t, 4H, J = 6.0 Hz, –CH$_2$–CH$_2$–O–), 7.62 (d, 4H, J = 10.0 Hz, Ar–H), 7.62 (d, 4H, J = 10.0 Hz, Ar–H), and 7.79 (s, 2H, –N–CH–). ^{13}C NMR (CDCl$_3$): δ 13.78, 18.31, 20.94, 23.91, 24.37, 26.33, 26.40, 29.42, 42.13, 46.74, 61.14, 66.18, 98.13, 109.00, 109.79, 119.65, 125.21, 126.80, 128.90, 131.10, 147.93, 174.11. FTIR: $\nu_{C–H}$ 2800–3000 cm^{-1}, $\nu_{Pt–C≡C}$ 2099 cm^{-1}, $\nu_{C=O}$ 1723 cm^{-1}, $\nu_{C=C \ Ar}$ 1608 cm^{-1}, $\nu_{C–O–C–O–C}$ 1079 cm^{-1}, $\nu_{1,4-disubst. \ benzene}$ 842 cm^{-1}, $\nu_{C–O–C–O–C}$ 828 cm^{-1}. MALDI-TOF: calculated M_w + Na$^+$ = 1386.61 g mol^{-1}, found M_w + Na$^+$ = 1386.77 g mol^{-1}.

4-Azidobenzyl alcohol (4). 4-Bromobenzyl alcohol (1.0 g; 5.34 mmol), sodium azide (0.87 g; 13.36 mmol), CuI (0.10 g; 0.53 mmol), L-proline (0.184 g; 1.60 mmol) and sodium hydroxide (64 mg; 1.60 mmol) were dissolved in 10 mL of ethanol–water (70 : 30). The reaction was run at 95 °C for 24 h. Additional water (5 mL) was added and the reaction was stirred for another 30 min. The water solution was extracted 3 times with ether. The collected organic phases were then extracted twice with water and twice with NaHSO$_4$ (10%). Finally the organic phase was dried with $MgSO_4$ and solvents were evaporated off. Yield 78%. ^{1}H NMR (CDCl$_3$): δ 2.79 (s, 1H, –OH), 4.56 (s, 2H, –CH$_2$–), 6.97 (d, 2H, J = 8.8 Hz, Ar–H), 7.28 (d, 2H, J = 8.8 Hz, Ar–H). ^{13}C NMR (CDCl$_3$): δ 64.31, 118.93, 128.38, 137.40, 139.14.

Triazole formation (5). The synthesis was conducted according to the general procedure for triazole formation as described above. Yield 22%. ^{1}H NMR (DMSO): δ 4.29 (s, 1H, –C≡C–H), 4.59 (d, 2H, J = 4.0 Hz, –CH$_2$–), 5.38 (t, 1H, J = 4 Hz, –OH), 7.56 (d, 2H, J = 8.0 Hz, Ar–H), 7.61 (d, 2H, J = 8.0 Hz, Ar–H), 7.90 (d, 2H, J = 8.0 Hz, Ar–H), 7.96 (d, 2H, J = 8.0 Hz, Ar–H), 9.35 (s, 1H, –N–CH–). ^{13}C NMR (DMSO): δ 62.13, 81.58, 83.26, 119.72, 120.13, 125.35, 127.59, 129.79, 130.61, 132.34, 135.08, 143.34, 146.37.

General procedure for anhydride coupling, exemplified with the synthesis of compound 6. Alcohol **5** (200 mg; 0.73 mmol) and 4-dimethylaminopyridine (DMAP, 20 mg; 0.16 mmol) were dissolved in 10 mL of pyridine. Acetonide protected bis-MPA anhydride (0.72 g; 2.2 mmol) was dissolved in 3 mL DCM and added to the reaction mixture. The reaction was stirred at room temperature overnight. The residual anhydride

was quenched with 5 mL of water under rigorous stirring for a couple of hours. Solvents were evaporated and the crude reaction mixture was redissolved in DCM. The organic phase was extracted 3 times with $NaHSO_4$ (10%), 3 times with Na_2CO_3 (10%), and finally once with brine. The organic phase was dried with $MgSO_4$ and purified by flash chromatography, eluting with heptane, gradually increasing to 50 : 50 ethyl acetate–heptane. Yield 95%. ^{1}H NMR ($CDCl_3$): δ 1.16 (s, 3H, $-CH_2-C-CH_3$), 1.36 (s, 3H, $O-C-CH_3$), 1.41 (s, 3H, $O-C-CH_3$), 3.16 (s, 1H, $-C\equiv C-H$), 3.67 (d, 2H, $J = 12.0$ Hz, $-C-CH_2-O-$), 4.22 (d, 2H, $J = 12.0$ Hz, $-C-CH_2-O-$), 5.24 (s, 2H, $Ar-CH_2-$), 7.34 (d, 2H, $J = 12.0$ Hz, $Ar-H$), 7.51 (d, 2H, $J = 12.0$ Hz, $Ar-H$), 7.76 (m, 4H, $Ar-H$), 8.15 (s, 1H, $-N-CH-$). ^{13}C NMR ($CDCl_3$): δ 18.29, 21.64, 25.41, 41.90, 65.90, 78.09, 83.36, 98.07, 117.79, 120.54, 122.09, 125.61, 129.09, 130.36, 132.66, 136.52, 136.98, 147.67, 173.98.

Platinum coupling (Z2). The synthesis was conducted according to the general procedure for platinum coupling as described above. Yield 90%. ^{1}H NMR ($CDCl_3$): δ 0.93 (t, 18H, $J = 8.0$, $-CH_2-CH_3$), 1.16 (s, 3H, $-CH_2-C-CH_3$), 1.36 (s, 3H, $O-C-CH_3$), 1.41 (s, 3H, $O-C-CH_3$), 1.43 (m, 12H, $-CH_2-CH_3$), 1.62 (m, 12H, $CH_2-CH_2-CH_3$), 2.15 (m, 12H, $-P-CH_2-$), 3.67 (d, 4H, $J = 12.0$ Hz, $-C-CH_2-O-$), 4.22 (d, 4H, $J = 12.0$ Hz, $-C-CH_2-O-$), 5.24 (s, 4H, $Ar-CH_2-$), 7.34 (d, 4H, $J = 12.0$ Hz, $Ar-H$), 7.51 (d, 4H, $J = 12.0$ Hz, $Ar-H$), 7.76 (m, 8H, $Ar-H$), 8.15 (s, 2H, $-N-CH-$). ^{13}C NMR ($CDCl_3$): δ 13.73, 18.34, 21.68, 23.87, 24.30, 25.40, 26.27, 30.19, 41.94, 65.40, 65.96, 98.01, 116.95, 120.35, 125.28, 125.30, 126.30, 128.09, 128.98, 131.08, 131.10, 135.64, 136.62, 148.49, 173.89. FTIR: ν_{C-H} 2800–3000 cm^{-1}, $\nu_{Pt-C\equiv C}$ 2095 cm^{-1}, $\nu_{C=O}$ 1740 cm^{-1}, $\nu_{C=C \ Ar}$ 1608 cm^{-1}, $\nu_{C-O-C-O-C}$ 1074 cm^{-1}, $\nu_{1,4\text{-disubst. benzene}}$ 845 cm^{-1}, $\nu_{C-O-C-O-C}$ 828 cm^{-1}. MALDI-TOF: calculated $M_w + Na^+ = 1482.70$ g mol^{-1}, found $M_w + Na^+ = 1482.87$ g mol^{-1}.

Synthesis of compound 7. Alkyne **3** (1.62 g, 4.23 mmol) was dissolved in 30 mL of TEA–pyridine (50 : 50). PPh_3 (66.5 mg; 0.25 mmol), CuI (20.1 mg; 0.106 mmol), $Pd(PPh_3)_2Cl_2$ (59.4 mg; 84.6 μmol) was added and the solution was heated to 120 °C. (4-Iodophenylethynyl)trimethylsilane (1.27 g; 4.23 mmol) was dissolved in 3 mL of TEA–pyridine and added dropwise to the heated solution. The reaction was refluxed for 2 h and followed by TLC. When complete, solvents were evaporated off and the crude mixture redissolved in DCM. The organic solution was extracted three times with $NaHSO_4$ (10%), dried with $MgSO_4$, and concentrated. The product was further purified by flash chromatography, eluting with heptane, gradually increasing to 40 : 60 ethyl acetate–heptane. Yield: 80%. ^{1}H NMR ($CDCl_3$): δ 0.25 (s, 9H, $-Si-CH_3$), 1.11 (s, 3H, $-CH_2-C-CH_3$), 1.38 (s, 3H, $O-C-CH_3$), 1.45 (s, 3H, $O-C-CH_3$), 2.35 (m, 2H, $-CH_2-CH_3$), 3.69 (d, 2H, $J = 12.0$ Hz, $-C-CH_2-O-$), 4.22 (d, 2H, $J = 12.0$ Hz, $-C-CH_2-O-$), 4.23 (t, 2H, $J = 6.0$ Hz, $-CH_2-CH_2-O-$), 4.53 (t, 2H, $J = 6.0$ Hz, $-N-CH_2-$), 7.45 (m, 4H, $Ar-H$), 7.57 (d, 2H, $J = 8.0$ Hz, $Ar-H$), 7.82 (d, 2H, $J = 8.0$ Hz, $Ar-H$), 7.88 (s, 1H, $-N-CH-$). ^{13}C NMR ($CDCl_3$): δ −0.10, 18.28, 20.67, 26.73, 29.00, 29.40, 42.18, 46.99, 61.06, 66.22, 89.86, 91.10, 96.33, 98.12, 104.45, 120.52, 122.58, 122.88, 123.19, 125.57, 130.53, 131.34, 131,87, 132.08, 174.16.

Deprotection of TMS (8). Compound **7** (1.89 g; 3.40 mmol) was dissolved in 100 mL THF, whereafter tetrabutylammonium fluoride (TBAF, 1 M solution in THF, 4.1 mL; 4.09 mmol) was added dropwise. The deprotection was allowed to proceed at room temperature for 1 h, followed by TLC. When complete, THF was evaporated off and the crude mixture redissolved in ethyl acetate and extracted three times with $NaHCO_3$. The organic phase was dried with $MgSO_4$ and concentrated. The product was further purified by flash chromatography, eluting with ethyl acetate–heptane starting from 20 : 80 and gradually increasing to 40 : 60. Yield: 72%. ^{1}H NMR ($CDCl_3$): δ 1.12 (s, 3H, $-CH_2-C-CH_3$), 1.38 (s, 3H, $O-C-CH_3$), 1.45 (s, 3H, $O-C-CH_3$), 2.35 (m, 2H, $-CH_2-CH_2-O-$), 3.17 (s, 1H, $-C\equiv C-H$), 3.66 (d, 2H, $J = 12.0$ Hz, $-C-CH_2-O-$), 4.21 (d, 2H, $J = 12.0$ Hz, $-C-CH_2-O-$), 4.22 (t, 2H, $J = 6.0$ Hz, $-N-CH_2-$), 4.53 (t, 2H, $J = 6.0$ Hz, $-CH_2-CH_2-O-$), 7.47 (s, 4H, $Ar-H$), 7.57 (d, 2H, $J = 8.0$ Hz, $Ar-H$), 7.82 (d, 2H, $J = 8.0$ Hz, $Ar-H$), and 7.86 (s, 1H, $-N-CH-$). ^{13}C NMR ($CDCl_3$): δ 18.30, 20.75, 26.65, 29.42, 42.18, 46.85, 61.06, 66.22, 78.94, 83.23, 89.62, 91.24, 98.18, 120.50, 121.89, 122.51, 123.65, 125.59, 130.61, 131.43, 132.04, 132.10, 147.05, 174.16.

Platinum coupling (Z3). The synthesis was conducted according to the general procedure for platinum coupling as described above. Yield 75%. ^{1}H NMR ($CDCl_3$): δ 0.91 (t, 18H, $J = 8.0$, $-CH_2-CH_3$), 1.10 (s, 6H, $-CH_2-C-CH_3$), 1.36 (s, 6H, $O-C-CH_3$), 1.44 (s, 6H, $O-C-CH_3$), 1.45 (m, 12H, $-CH_2-CH_3$), 1.60 (m, 12H, $CH_2-CH_2-CH_3$), 2.12 (m, 12H, $-P-CH_2-$), 2.33 (m, 4H, $-CH_2-CH_2-O-$), 3.66 (d, 4H, $J = 12.0$ Hz, $-C-CH_2-O-$), 4.21 (d, 4H, $J = 12.0$ Hz, $-C-CH_2-O-$), 4.22 (t, 4H, $J = 6.0$ Hz, $-N-CH_2-$), 4.51 (t, 4H, $J = 6.0$ Hz, $-CH_2-CH_2-O-$), 7.22 (d, 4H, $J = 8.0$ Hz, $Ar-H$), 7.37 (d, 4H, $J = 8.0$ Hz, $Ar-H$), 7.55 (d, 4H, $J = 8.0$ Hz, $Ar-H$), 7.79 (d, 4H, $J = 8.0$ Hz, $Ar-H$), and 7.84 (s, 2H, $-N-CH-$). ^{13}C NMR ($CDCl_3$): δ 13.71, 18.21, 20.73, 23.85, 24.29, 26.25, 26.52, 29.32, 42.08, 46.76, 61.00, 66.12, 77.20, 89.64, 90.84, 98.07, 109.27, 119.01, 120.35, 123.09, 125.46, 129.06, 130.02, 130.58, 131.11, 131.81, 147.05, 174.05. FTIR: ν_{C-H} 2800–3000 cm^{-1}, $\nu_{Pt-C\equiv C}$ 2094 cm^{-1}, $\nu_{C=O}$ 1736 cm^{-1}, $\nu_{C=C \ Ar}$ 1595 cm^{-1}, $\nu_{C-O-C-O-C}$ 1077 cm^{-1}, $\nu_{1,4\text{-disubst. benzene}}$ 846 cm^{-1}, $\nu_{C-O-C-O-C}$ 832 cm^{-1}. MALDI-TOF: calculated $M_w + Na^+ = 1586.85$ g mol^{-1}, found $M_w + Na^+ = 1586.89$ g mol^{-1}.

Results and discussion

Various structures of platinum(II) acetylides based on aromatic alkynes have been synthesized and thoroughly characterized previously.[23,36,37] However, reports on platinum(II) acetylides prepared by click chemistry are rare. In this study triazole units were incorporated at three different positions in an NLO chromophore in order to evaluate how the position of the triazole affects the OPL properties of these chromophores. The three molecules are illustrated in Scheme 1. The smallest molecule in the study, **Z1**, contains a short conjugation path length, with the triazole unit at the end of the conjugation. This molecule resembles the previously investigated platinum(II) acetylide[20] (**Pt1-G1**) with the difference of a triazole instead of an ethynyl-phenyl group. The **Z2** molecule has the triazole unit in between two aromatic rings. The **Z3**
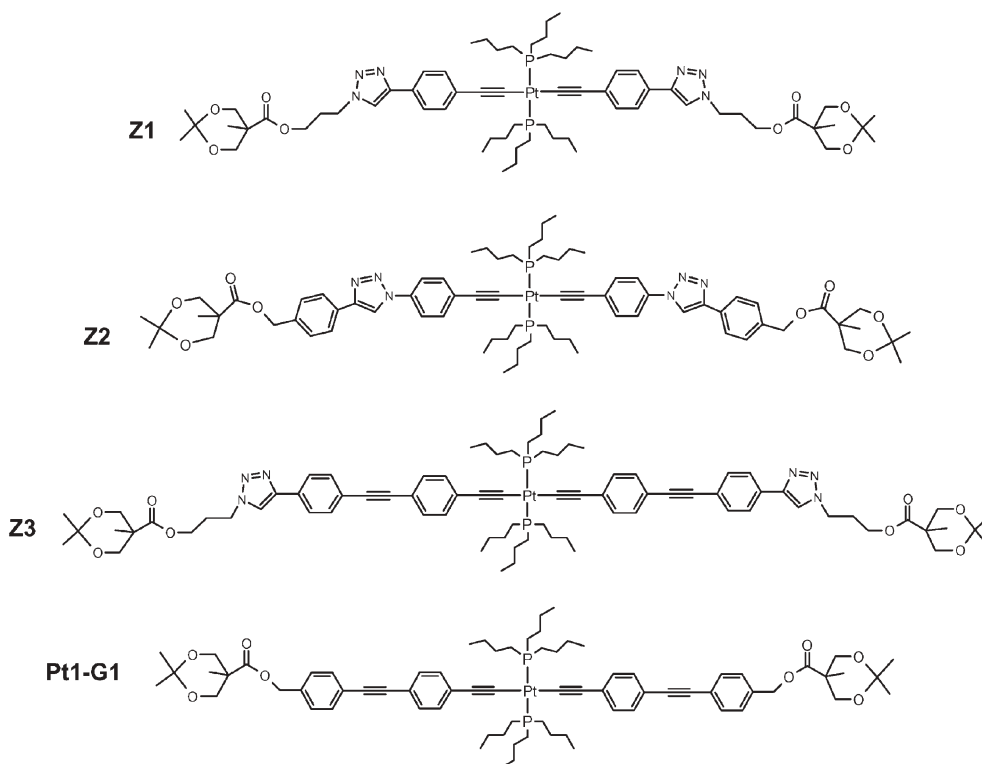
Scheme 1 Chemical structures of the triazole-containing platinum(II) acetylides, **Z1**, **Z2,** and **Z3**, and the previously studied **Pt1-G1**.

molecule has a more extended conjugation than the previous two, and the triazole unit is located at the end of the conjugation. These molecules were chosen to evaluate whether the triazole contributes to the conjugation and participates in the electron transfer. The **Z2** molecule was examined to investigate whether the triazole disrupts the conjugation over the aromatics, or if efficient electron transfer can be achieved through the triazole.
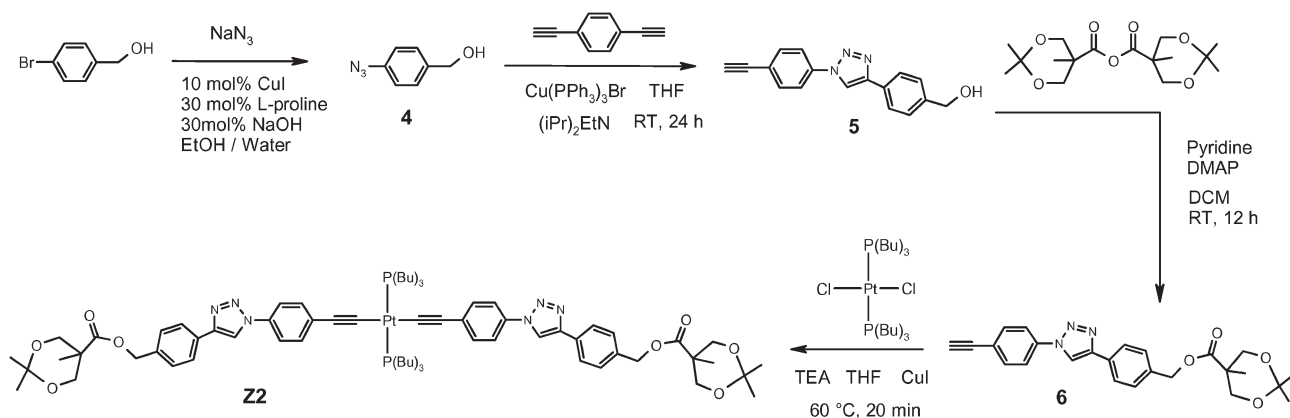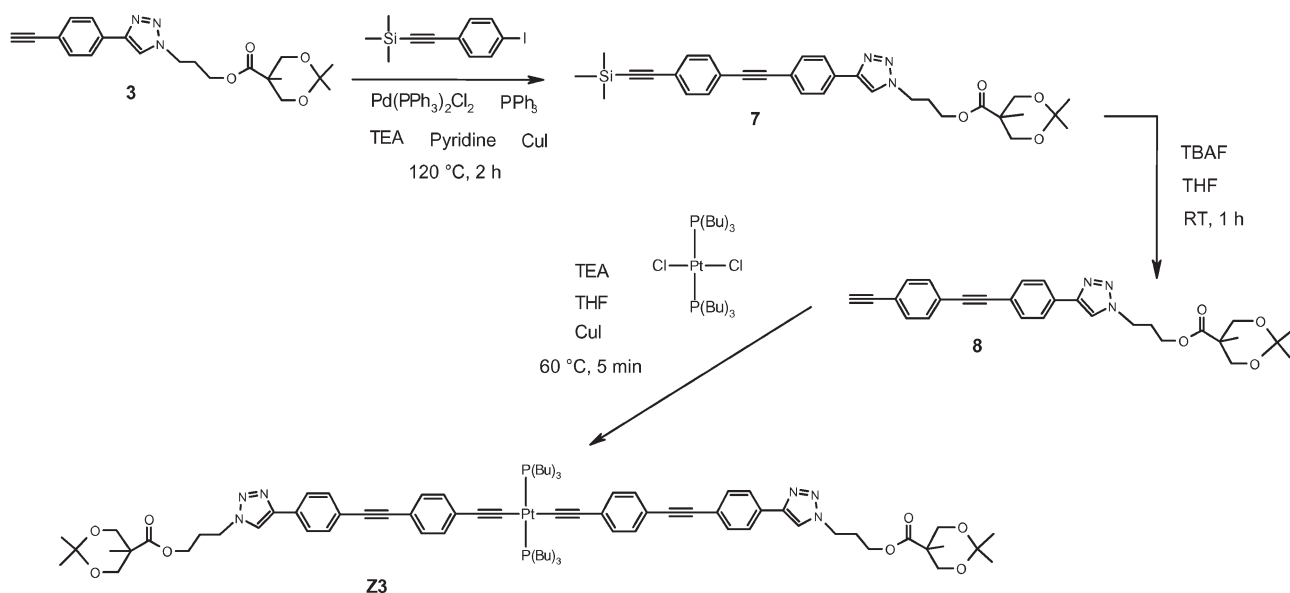
Synthesis of molecules

The **Z1** molecule was synthesized by coupling a chloro-functional spacer to the acetonide protected bis-MPA followed by substitution of the chloride to an azide. At this point larger dendrons can be grown divergently using the iterative

procedure of deprotection and subsequent addition of the acetonide protected bis-MPA anhydride according to the literature.[33] The azide-functional acetonide protected bis-MPA was then coupled to di-ethynyl benzene through click chemistry, creating a triazole-containing phenyl-ethynyl arm. Finally, the triazole-modified phenyl-ethynyl arms were coupled to a platinum salt by Sonogashira coupling to obtain the final **Z1** molecule (Scheme 2).

The synthesis of **Z2** is somewhat different from the approach to **Z1**. The **Z2** molecule was prepared by adding sodium azide[38] to bromobenzyl alcohol[39] and subsequent cyclo-addition of the azide with diethynyl benzene. The hydroxy functionality was then reacted with the acetonide protected bis-MPA anhydride to accomplish a generation 1 alkyne arm. As for **Z1**, the final **Z2** chromophore was
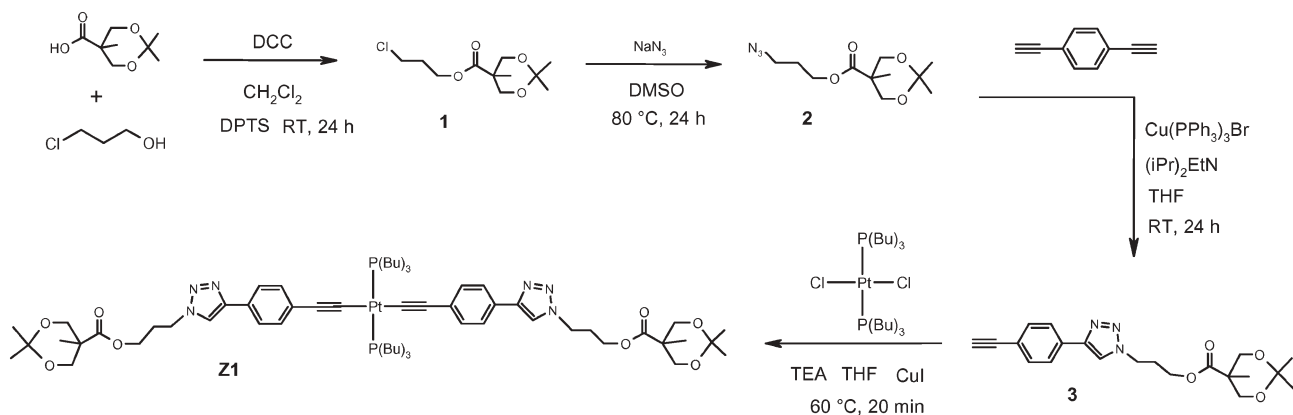
Scheme 2 Synthesis of chromophore **Z1**.

Scheme 3 Synthesis of chromophore **Z2**.

Scheme 4 Synthesis of chromophore **Z3**.

obtained by Sonogashira coupling to the platinum salt (Scheme 3).

The **Z3** molecule was synthesized in a similar manner to **Z1** and **Z2** (Scheme 4). All click reactions were conducted using an alkyl azide and a difunctional ethynyl compound in a 1 : 1 equivalents ratio. Hence, the aim was only for the monosubstituted product; however, various amounts of the disubstituted product were also formed. The yields for the monosubstituted triazole formation products were up to 90%. As mentioned in the introduction, click reactions are associated with high yields, and highly pure products where column chromatography purification is not necessary. However, considering the circumstances with the difunctional ethynyl reagent, formation of disubstituted product will be inevitable and column chromatography is needed to isolate the monosubstituted product.

Photo-physical characterization

Fig. 2 shows linear absorption spectra for the three final chromophores. The spectra of **Z1** and **Z2** are almost identical,
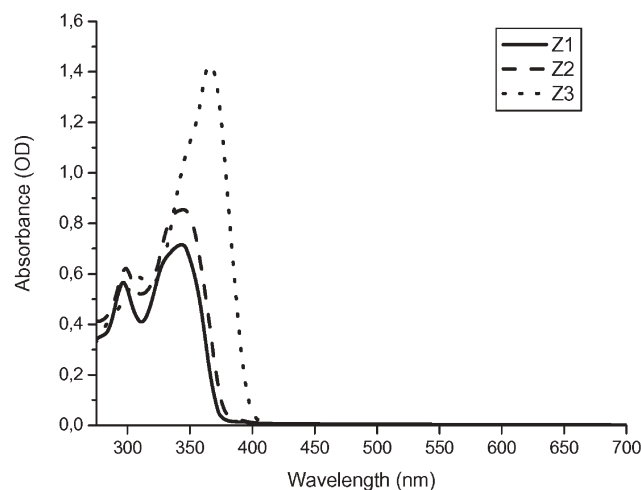

Fig. 2 Linear absorption spectra for **Z1**, **Z2** and **Z3** (10 μM solutions in THF).

Table 1 Absorption peaks, emission peaks, extinction coefficient, quantum yield and excited state lifetimes of the three investigated compounds

Molecule	Absorption peaks/nm	Emission peaks/nm	Extinction coeff./10^4 M^{-1} cm^{-1}, and quantum yield	Fluorescence and phosphorescence lifetimes[a]
Z1	(296), 342	388, 486	7.1, <0.001[b]	1–10 ps, 50 ns
Z2	(298), 342	388, 488	8.5, <0.001[b]	1–10 ps, 76 ns
Z3	(308), 365	396, 535	14.3, ⩽0.001	1–10 ps, 260 ns

[a] Phosphorescence lifetimes measured in oxygen saturated samples. Longer lifetimes are obtained for oxygen evacuated samples (see text).
[b] Very weak fluorescence signal; the quantum yield values were not possible to determine more accurately.

exhibiting two absorption bands, one weak band at 296 nm and a stronger band at 342 nm. The minor peak for the **Z3** molecule is red-shifted by approximately 10 nm, giving rise to a weak band at 308 nm, whereas the major peak is red-shifted by 23 nm and peaks at 365 nm (very similar to the spectrum of the previously investigated platinum(II) acetylides without triazole units[18,20]). The red-shift is most likely due to the extended conjugation in the **Z3** molecule. The large peak for all compounds corresponds to the singlet–singlet transition ($S_0 \rightarrow S_1$). Absorption peak wavelengths and extinction coefficients are summarized in Table 1.

The similarity of the **Z1** and **Z2** molecules indicates that the electron transfer over the triazole unit in the **Z2** molecule is in fact interrupted by the triazole unit. Otherwise, the absorption bands for **Z2** would most likely also be red-shifted as for the **Z3** molecule. Transmission spectra show that all three molecules possess high linear transmission above 400 nm.

Luminescence spectra and excited state decay lifetimes were also recorded for all three molecules (Fig. 3). Two distinct bands were observed in the luminescence spectrum for all chromophores. The band that peaks at around 390 nm results from radiative relaxation from $S_1 \rightarrow S_0$ and is denoted fluorescence due to its short life-time. The second band that peaks around 490 nm for **Z1** and **Z2**, and around 535 nm for **Z3**, is associated with phosphorescence from $T_1 \rightarrow S_0$ (through intersystem crossing (ISC) from $S_1 \rightarrow T_n$) due to its long life-time. The intersystem crossing is greatly increased by the platinum atom which enhances the spin–orbit

coupling for these chromophores and thus allows long-lived phosphorescence. Interestingly, **Z1** and **Z2** show fairly weak fluorescence bands, whereas **Z3** emit more efficiently at a slightly higher wavelength band around 400 nm. The phosphorescence bands are equally weak for all chromophores in oxygen saturated solutions. However, the phosphorescence peak for **Z3** is red-shifted by almost 50 nm.

Fluorescence decay times were found to be very short. For all three compounds they were found to be below 10 ps. The phosphorescence decay times (single component) were measured to be between 50–260 ns in oxygen saturated samples (Table 1) with representative decay curves as shown in Fig. 4. The fluorescence quantum efficiency for all compounds, **Z1**, **Z2** and **Z3**, was found to be very small. They were all estimated to be below 10^{-3}, which is in the same order of magnitude as the previously investigated **Pt1-G1**.[17] With our experimental set-up it was not possible to determine the values more accurately. However, we could see that the values for **Z1** and **Z2** were comparable and somewhat lower than those of **Z3** and **Pt1-G1** (data not shown). The low fluorescence emission is explained by the very efficient ISC to the triplet manifold for such heavy-atom containing chromophores.[37,40]

The triplet state is almost totally quenched by the presence of oxygen in the solution, therefore the total amount of "visible" triplet luminescence from these samples is very low. It was shown by Lindgren et al.[17] that bright phosphorescence from, e.g., **Pt1-G1** can be obtained by removing the dissolved oxygen in the sample using a series of freeze–thaw cycles under
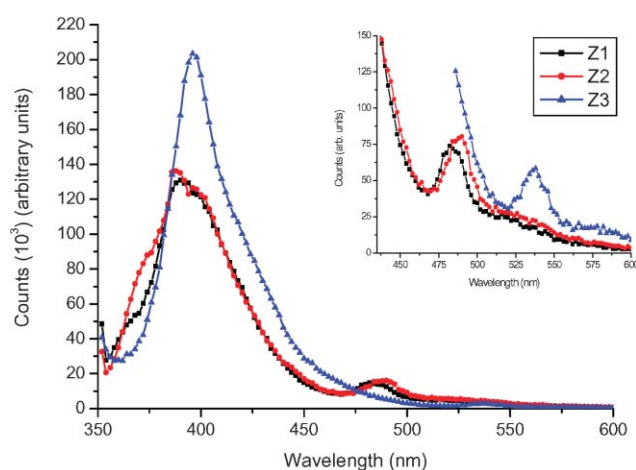
Fig. 3 Luminescence spectra for **Z1**, **Z2** and **Z3**. Excitation wavelength at 350 nm at 4.75 MHz prf. Samples diluted to 10 μM in THF solvent. The inset shows the right wing of the spectrum on a different scale in order to show the phosphorescence bands more clearly.
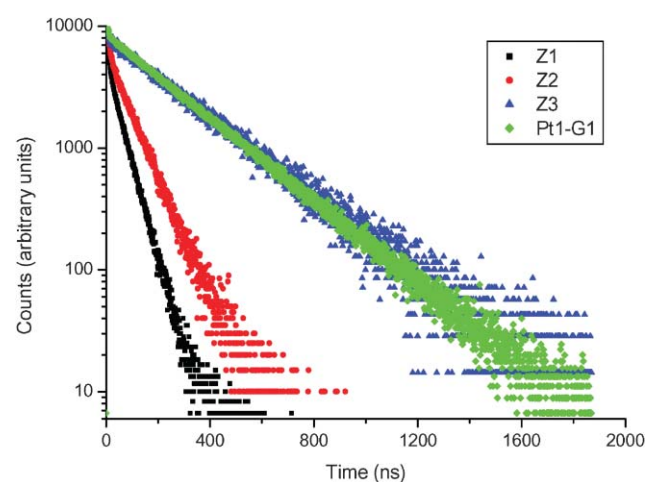
Fig. 4 Phosphorescence lifetime decay curves for **Z1**, **Z2** and **Z3** in oxygen saturated samples. Decay of the previously studied **Pt1-G1** is shown for comparison. Excitation wavelength at 360 nm, and 500 kHz prf. All samples in approximately 10 μM THF solutions.
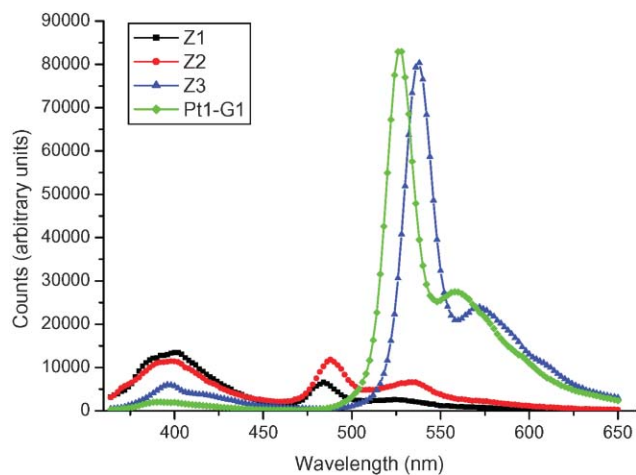
Fig. 5 Bright phosphorescence from 10 μM samples purged with argon gas. Large double peaks are shown for both **Z3** and **Pt1-G1** (527, 556 nm, and 538, 573 nm, respectively). Also some enhancement of the phosphorescence peaks for **Z1** and **Z2** is shown, compared to Fig. 3.

vacuum. The bright phosphorescence that then appears showed a decay time in the order of 100 μs, a value three orders of magnitude larger than the oxygen saturated decay time. In this study it was found that the same result could be achieved by bubbling argon gas through the sample for 10–15 min, hence displacing most of the oxygen dissolved in the solution. Thus, when the samples of **Z1**, **Z2**, **Z3**, and **Pt1-G1** were purged with argon gas, bright green visible phosphorescence appeared (Fig. 5). At the same time the phosphorescence decay times for both **Pt1-G1** and **Z3** were increased to approximately 100 μs (data not shown), in accordance with the previously obtained results for the Pt-capped dendrimers.[17] Interestingly, for **Z1** and **Z2** the procedure with argon purging was not as successful as for **Z3** and **Pt1-G1** even though the experiments were carried out under identical conditions. Thus, the detailed molecular structure must also be of importance for the quenching of triplet states. Even if the observed effect was not as large for **Z1** and **Z2**, still an enhancement of the amount of phosphorescence was observed together with a significant increase in the phosphorescence lifetime to approximately 6 μs for both **Z1** and **Z2** (data not shown).

By the same method as above, an estimation of the phosphorescence emission quantum efficiency was performed. These measurements were performed on samples where a significant part of the dissolved oxygen was removed by argon-gas purging (Fig. 5). The phosphorescence quantum efficiency, as defined here, contains both the ISC factor and the phosphorescence emission yield; hence, it is a product of the two factors. The measurement gave approximate values of 0.04 and 0.05 for **Z3** and **Pt1-G1**, respectively. These values are significantly higher than the fluorescence quantum yields, showing that the ISC process must be a very efficient process. For **Z1** and **Z2** the values are one order of magnitude lower, in the order of 10^{-3}. Taking into account that in all samples some triplet states may still be oxygen quenched (since the argon-gas purging is not assumed to completely remove the dissolved

oxygen, even for **Z3** and **Pt1-G1**) the ISC channel is verified as the main output channel from the first excited singlet state. This is in agreement with the de-excitation process previously proposed by Lindgren *et al.*[17]

Multiphoton absorption

The emission upon two-photon absorption (TPA) was also recorded as shown in Fig. 6. The molecules were excited at approximately twice the wavelength of their linear absorption maximum, and consequently two photons are needed to excite the electrons to higher excited states, whereafter the radiative relaxation of these transitions was analyzed. All spectra show the same trends as in the one-photon excitation case. The emission measurements from TPA display very weak fluorescence and phosphorescence for **Z1** and **Z2** (just as in the one-photon case). In contrast, **Z3** shows greater fluorescence and phosphorescence in the TPA luminescence measurements, compared to the other two compounds. The two-photon absorption process will have a quadratic dependence on the incoming intensity. Therefore the amount of two-photon excited fluorescence will also have this intensity dependence on excitation. A logarithmic plot of the fluorescence emission *vs.* the logarithm of the peak laser intensity will theoretically give a straight line with a gradient of two. Such a plot of the measured fluorescence emission for compound **Z3** is shown in Fig. 7. With a linear gradient of 1.96 it is very close to the expected value. This shows that we indeed have two-photon absorption. There are also some uncertainties due to random fluctuations because of the low fluorescence signal in this case. The pulse repetition frequency was 4.75 MHz. Even though this is high, it does not seem to interfere with the triplet-energy levels and ESA from the triplet states since we are monitoring the fluorescence directly from the singlet manifold.

An estimation of the TPA cross section can be made from the luminescence spectrum obtained for **Z3** compared to the spectrum for coumarin 110 (data not shown). Also, since the quantum efficiency was not found very accurately, it is convenient to give the value for the product of fluorescence quantum efficiency φ and TPA cross section σ_2. This is found
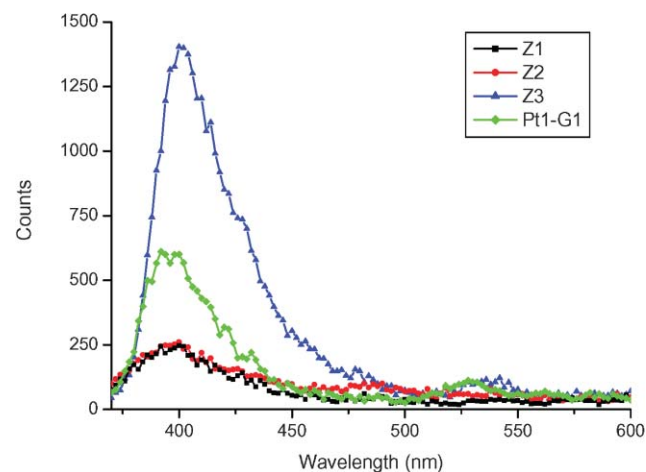
Fig. 6 Two-photon emission spectra for **Z1**, **Z2** and **Z3** (and **Pt1-G1**). Excitation wavelength is 720 nm. 200 kHz pulse repetition frequency. Samples in 50 μM solutions dissolved in THF.
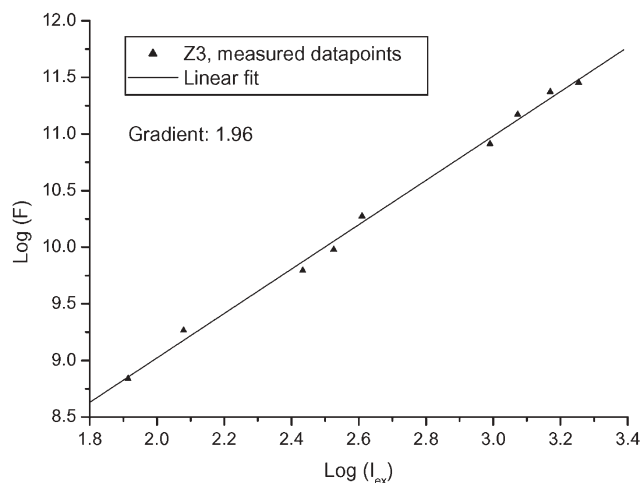
Fig. 7 Graph showing two-photon excited fluorescence *vs.* laser intensity (log–log plot) for the **Z3** compound (sample concentration is approx. 10 μM in THF). The excitation wavelength was set to 750 nm at 4.75 MHz prf.

to be in the order of 0.020 GM, that is, a cross section of minimum 20 GM if the upper limit of the quantum efficiency is taken to be 0.001. This result gives a value for the TPA cross section for **Z3** that is a little larger, but still on the same order of magnitude as the value for **Pt1-G1** obtained previously.[17] Therefore, this indicates that the extended conjugation, along with the triazole, may have a small contribution to the ability for two photon absorption of these molecules.

Optical power limiting

Optical power limiting measurements at 532 nm show that all three molecules possess good optical limiting ability and reach fairly low clamping levels (Fig. 8). **Z1** is the least efficient of the three, with an output of 8 μJ for 200 μJ input energy (91% linear absorption at 532 nm). **Z2** reaches down to 5.5 μJ output energy for 200 μJ input energy (69% linear transmission at 532 nm). **Z3** gives the best OPL response reaching down to a clearly defined clamping level of 2.5 μJ
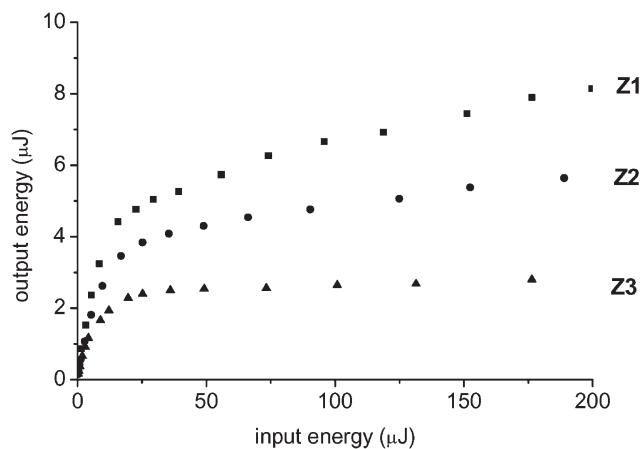
Fig. 8 Optical power limiting measurements showing input energy *versus* transmitted (output) energy at 532 nm for **Z1**, **Z2** and **Z3** (50 mM solutions in THF).

(80% linear transmission at 532 nm). It is believed that the extended conjugation combined with the triazole end-functionalities of the **Z3** chromophore are responsible for the improved OPL response due to efficient electron transfer and strong excited state absorption. In comparison, these clamping levels were similar to or better than the optical power limiting results of previously investigated chromophores, such as zinc based porphyrins reaching a clamping level of 6 μJ, and dendronized bis(phenylethynyl)thiophenes reaching clamping levels in the range of 8–15 μJ (for samples with three times higher concentration).[5,6] The triazole-functionalized chromophore, **Z3** (with a clamping level of 2.5 μJ), also performed better than the predecessor **Pt1-G1** chromophore which reached a clamping level of 3.3 μJ.

Conclusions

It has been shown that triazole-functionalized platinum(II) acetylides, targeted for OPL applications, can be synthesized by click chemistry. Furthermore, utilizing click chemistry does offer an alternative route to the preparation of dendronized (bis-MPA) platinum(II) acetylide chromophores. The bis-MPA end-group on NLO chromophores has several benefits. Firstly, it acts as model compound proving that similar procedures can be used to obtain chromophores with larger dendritic substituents. Hence, adding larger dendritic substituents will increase the site isolation and thus improve the optical power limiting. Secondly, the bis-MPA unit facilitates the solubility of the platinum(II) acetylide chromophore in many organic solvents, and prevents π-stacking of chromophores. Aggregation of chromophores is unwanted due to the decrease in linear transmission that clusters may cause. Moreover, the bis-MPA unit may be beneficial for further functionalization of the chromophore,[20] offering multiple reaction sites available for further modification.

Photophysical characterization show that the triazole units do contribute to the nonlinear optical properties of these molecules; however, the most important factor for efficient power limiting is due to extended conjugation together with spin–orbit coupling offered by the platinum atom. Optical power limiting measurements show that all compounds (**Z1**, **Z2** and **Z3**) possess good limiting abilities. The best clamping level was reached for the **Z3** molecule due to its extended conjugation and placement of the triazole units at the end of the conjugation.

Acknowledgements

References

1 S. Sanders, *Opt. Photonics News*, 2005, **16**, 36–41.

2 C. W. Spangler, *J. Mater. Chem.*, 1999, **9**, 2013–2020.

3 C. Li, C. Liu, Q. Li and Q. Gong, *Chem. Phys. Lett.*, 2004, **400**, 569–572.

4 R. C. Hollins, *Curr. Opin. Solid State Mater. Sci.*, 1999, **4**, 189–196.

5 R. Vestberg, A. Nyström, M. Lindgren, E. Malmström and A. Hult, *Chem. Mater.*, 2004, **16**, 2794–2804.

6 R. Vestberg, C. Nilsson, C. Lopes, P. Lind, B. Eliasson and E. Malmström, *J. Polym. Sci., Part A: Polym. Chem.*, 2005, **43**, 1177–1187.

7 J. W. Baur, M. D. Alexander, Jr., M. Banach, L. R. Denny, B. A. Reinhardt, R. A. Vaia, P. A. Fleitz and S. M. Kirkpatrick, *Chem. Mater.*, 1999, **11**, 2899–2906.

8 J. E. Ehrlich, X. L. Wu, I. Y. S. Lee, Z. Y. Hu, H. Rockel, S. R. Marder and J. W. Perry, *Opt. Lett.*, 1997, **22**, 1843–1845.

9 G. S. He, G. C. Xu, P. N. Prasad, B. A. Reinhardt, J. C. Bhatt and A. G. Dillard, *Opt. Lett.*, 1995, **20**, 435–437.

10 T. J. McKay, J. Staromlynska, P. Wilson and J. Davy, *J. Appl. Phys.*, 1999, **85**, 1337–1341.

11 R. Kannan, G. S. He, T.-C. Lin, P. N. Prasad, R. A. Vaia and L.-S. Tan, *Chem. Mater.*, 2004, **16**, 185–194.

12 C. E. Powell and M. G. Humphrey, *Coord. Chem. Rev.*, 2004, **248**, 725–756.

13 C.-H. Tao, N. Zhu and V. W.-W. Yam, *Chem.–Eur. J.*, 2005, **11**, 1647–1657.

14 N. Chawdhury, A. Koehler, R. H. Friend, M. Younus, N. J. Long, P. R. Raithby and J. Lewis, *Macromolecules*, 1998, **31**, 722–727.

15 J. Lewis, N. J. Long, P. R. Raithby, G. P. Shields, W.-Y. Wong and M. Younus, *J. Chem. Soc., Dalton Trans.*, 1997, 4283–4288.

16 R. Kannan, G. S. He, L. Yuan, F. Xu, P. N. Prasad, A. G. Dombroskie, B. A. Reinhardt, J. W. Baur, R. A. Vaia and L.-S. Tan, *Chem. Mater.*, 2001, **13**, 1896–1904.

17 M. Lindgren, B. Minaev, E. Glimsdal, R. Vestberg, R. Westlund and E. Malmström, *J. Lumin.*, 2007, **124**, 302–310.

18 R. Vestberg, R. Westlund, A. Eriksson, C. Lopes, M. Carlsson, B. Eliasson, E. Glimsdal, M. Lindgren and E. Malmström, *Macromolecules*, 2006, **39**, 2238–2246.

19 S. Parola, M. Oertenblad, F. Chaput, C. Desroches, P. Miele, P. L. Baldeck, E. Malmström, M. Lindgren, B. Eliasson, A. Eriksson and C. Lopes, *Proc. SPIE—Int. Soc. Opt. Eng.*, 2005, **5934**, 593404.

20 R. Westlund, E. Malmström, M. Hoffmann, R. Vestberg, C. Hawker, E. Glimsdal, M. Lindgren, P. Norman, A. Eriksson and C. Lopes, *Proc. SPIE—Int. Soc. Opt. Eng.*, 2006, **6401**, 64010H.

21 J. Staromlynska, P. B. Chapple, J. R. Davy and T. J. McKay, *Proc. SPIE—Int. Soc. Opt. Eng.*, 1994, **2229**, 59–66.

22 J. Staromlynska, T. J. McKay and P. Wilson, *J. Appl. Phys.*, 2000, **88**, 1726–1732.

23 T. J. McKay, J. A. Bolger, J. Staromlynska and J. R. Davy, *J. Chem. Phys.*, 1998, **108**, 5537–5541.

24 P. Furuta and J. M. J. Fréchet, *J. Am. Chem. Soc.*, 2003, **125**, 13173–13181.

25 H. Ma and A. K. Y. Jen, *Adv. Mater.*, 2001, **13**, 1201–1205.

26 H. C. Kolb, M. G. Finn and K. B. Sharpless, *Angew. Chem., Int. Ed.*, 2001, **40**, 2004–2021.

27 P. Wu, A. K. Feldman, A. K. Nugent, C. J. Hawker, A. Scheel, B. Voit, J. Pyun, J. M. J. Frechet, K. B. Sharpless and V. V. Fokin, *Angew. Chem., Int. Ed.*, 2004, **43**, 3928–3932.

28 M. Malkoch, K. Schleicher, E. Drockenmuller, C. J. Hawker, T. P. Russell, P. Wu and V. V. Fokin, *Macromolecules*, 2005, **38**, 3663–3678.

29 M. J. Joralemon, R. K. O'Reilly, J. B. Matson, A. K. Nugent, C. J. Hawker and K. L. Wooley, *Macromolecules*, 2005, **38**, 5436–5443.

30 B. Helms, J. Mynar, C. Hawker and J. M. Fréchet, *J. Am. Chem. Soc.*, 2005, **126**, 15020–15021.

31 A. T. R. Williams, S. A. Winfield and J. N. Miller, *Analyst*, 1983, **108**, 1067–1071.

32 E. Glimsdal, M. Carlsson, B. Eliasson, B. Minaev and M. Lindgren, *J. Phys. Chem. A*, 2007, **111**, 244–250.

33 M. Malkoch, E. Malmström and A. Hult, *Macromolecules*, 2002, **35**, 8307–8314.

34 R. Gujadhur, D. Venkataraman and J. T. Kintigh, *Tetrahedron Lett.*, 2001, **42**, 4791–4793.

35 J. S. Moore and S. I. Stupp, *Macromolecules*, 1990, **23**, 65–70.

36 M. I. Bruce, J. Davy, B. C. Hall, Y. J. Van Galen, B. W. Skelton and A. H. White, *Appl. Organomet. Chem.*, 2002, **16**, 559–568.

37 J. E. Rogers, T. M. Cooper, P. A. Fleitz, D. J. Glass and D. G. McLean, *J. Phys. Chem. A*, 2002, **106**, 10108–10115.

38 M. Peer, *Spec. Chem. Mag.*, 1998, **18**, 256–257; M. Peer, *Spec. Chem. Mag.*, 1998, **18**, 259; M. Peer, *Spec. Chem. Mag.*, 1998, **18**, 261; M. Peer, *Spec. Chem. Mag.*, 1998, **18**, 263.

39 W. Zhu and D. Ma, *Chem. Commun.*, 2004, 888–889.

40 J. E. Rogers, B. C. Hall, D. C. Hufnagle, J. E. Slagle, A. P. Ault, D. G. McLean, P. A. Fleitz and T. M. Cooper, *J. Chem. Phys.*, 2005, **122**, 214708.